View metadata, citation and similar papers at core.ac.uk

brought to you by CORE

provided by Elsevier - Publisher Connector

Structure 14, 451–456, March 2006 ©2006 Elsevier Ltd All rights reserved DOI 10.1016/j.str.2005.11.019

Crystal Structure of the Boronic Acid-Based Proteasome Inhibitor Bortezomib in Complex with the Yeast 20S Proteasome

Michael Groll,[1,*] Celia R. Berkers,[2] Hidde L. Ploegh,[3,4] and Huib Ovaa[3,5,*]

[1] Department for Physiological Chemistry
Ludwig-Maximilians-University
Butenandtstrasse 5, Building B 81377
München
Germany

[2] Division of Cellular Biochemistry
Netherlands Cancer Institute
Plesmanlaan 121
1066 CX Amsterdam
The Netherlands

[3] Harvard Medical School
77 Avenue Louis Pasteur
Boston, Massachusetts 02115

Summary

The dipeptide boronic acid bortezomib, also termed VELCADE®, is a proteasome inhibitor now in use for the treatment of multiple myeloma, and its use for the treatment of other malignancies is being explored. We determined the crystal structure of the yeast 20S proteasome in complex with bortezomib to establish the specificity and binding mode of bortezomib to the proteasome's different catalytically active sites. This structure should enable the rational design of new boronic acid derivatives with improved affinities and specificities for individual active subunits.

Introduction

The ubiquitin-proteasome pathway plays a central role in proteolysis (Groll et al., 2005; Hershko and Ciechanover, 1998). The proteolytic component of this system, the 26S proteasome, consists of two 19S regulatory particles (RPs), involved in substrate recognition and unfolding, and a core particle (CP) termed 20S proteasome. The CP possesses a unique barrel-shaped structure, which contains 28 protein subunits, arranged in 4 stacked rings, each subunit occupying unique locations within the molecule (Groll et al., 1997; Löwe et al., 1995). The outer α rings of the $\alpha_7\beta_7\beta_7\alpha_7$ complex interact with the RPs, whereas the two inner β rings harbor the proteolytically active sites. In eukaryotic proteasomes, three β-type subunits, β1, β2 and β5, contain proteolytically active centers (Groll et al., 1997). Catalytic activities of these active β-type subunits are associated with their N-terminal threonine residue, which acts as a nucleophile in hydrolysis, thus classifying proteasomes as members of the family of Ntn (N-terminal nucleophilic) hydrolases (Brannigan et al., 1995; Löwe et al., 1995). Proteasomes can cleave after most amino acids: proteolytic activity measured against fluorogenic substrates illustrates three distinct cleavage preferences, termed chymotryptic, tryptic, and caspase-like activities (Orlowski et al., 1993), which can roughly be assigned to the subunits β5, β2, and β1, respectively (Figure 1A) (Groll et al., 1999).

Since proteasomes are responsible for the cytoplasmic turnover of the vast majority of proteins, and are hence central to many cellular processes, the manipulation of proteasomal activity is a key goal in controlling the stability of regulatory proteins (Groll and Huber, 2004; Kisselev and Goldberg, 2001). While proteasome inhibitors have been used extensively as investigative tools, the observation that they cause apoptosis in certain tumor-derived cell lines has led to their application as potential cancer therapeutics (Adams et al., 1998). The proteasome inhibitor bortezomib has been approved for the treatment of multiple myeloma patients (Ludwig et al., 2005; Richardson et al., 2005; Teicher et al., 1999).

Although crystal structures of the proteasome CP complexed with peptide aldehyde-based inhibitors are known (Groll and Huber, 2004; Kisselev and Goldberg, 2001), the X-ray structure of bortezomib with the 20S proteasome has not been reported. Here, we establish the crystal structure of the yeast 20S proteasome in complex with bortezomib at 2.8 Å resolution. The structural data for the bortezomib-proteasome complex presented here explain the different in vivo binding affinities of bortezomib for the individual subunits at atomic resolution. Subunit specificities can roughly be attributed to interactions of the leucine, pyrazine, and boronate moieties. Our data provide opportunities for future drug improvement.

Results

Under physiological conditions, the dipeptide boronic acid bortezomib preferentially targets the proteasomal β5 active site and, to a lesser extent, the β1 site, while the β2 site is left relatively untouched (β5>β1>>β2) (Berkers et al., 2005). Analysis of the structure of the yeast 20S proteasome complexed with bortezomib shows all active sites occupied by the inhibitor, attributable to the high concentrations of the ligand (10 mM) used in the course of crystal soaking. The specificity pockets of individual active subunits do not only differ in charge pattern, but also in their overall architecture. Nevertheless, the binding mode of bortezomib to all three subunits is identical.

Binding to the Bortezomib Peptide Backbone

In its bound conformation, bortezomib adopts an antiparallel β sheet conformation (Figure 1B), filling the gap between strands S2 and S4. These β sheets are stabilized by direct hydrogen bonds between the conserved residues (Gly47N, Thr21N, Thr21O, and Ala49O) of the β-type subunits and main chain atoms of the drug

*Correspondence: mgroll@med.uni-muenchen.de (M.G.); h.ovaa@nki.nl (H.O.)

[4] Present address: Whitehead Institute of Biomedical Research, Massachusetts Institute of Technology, 9 Cambridge Centre, Room 345, Cambridge, Massachusetts 02142.

[5] Present address: Division of Cellular Biochemistry, Netherlands Cancer Institute, Plesmanlaan 121, 1066 CX Amsterdam, The Netherlands.

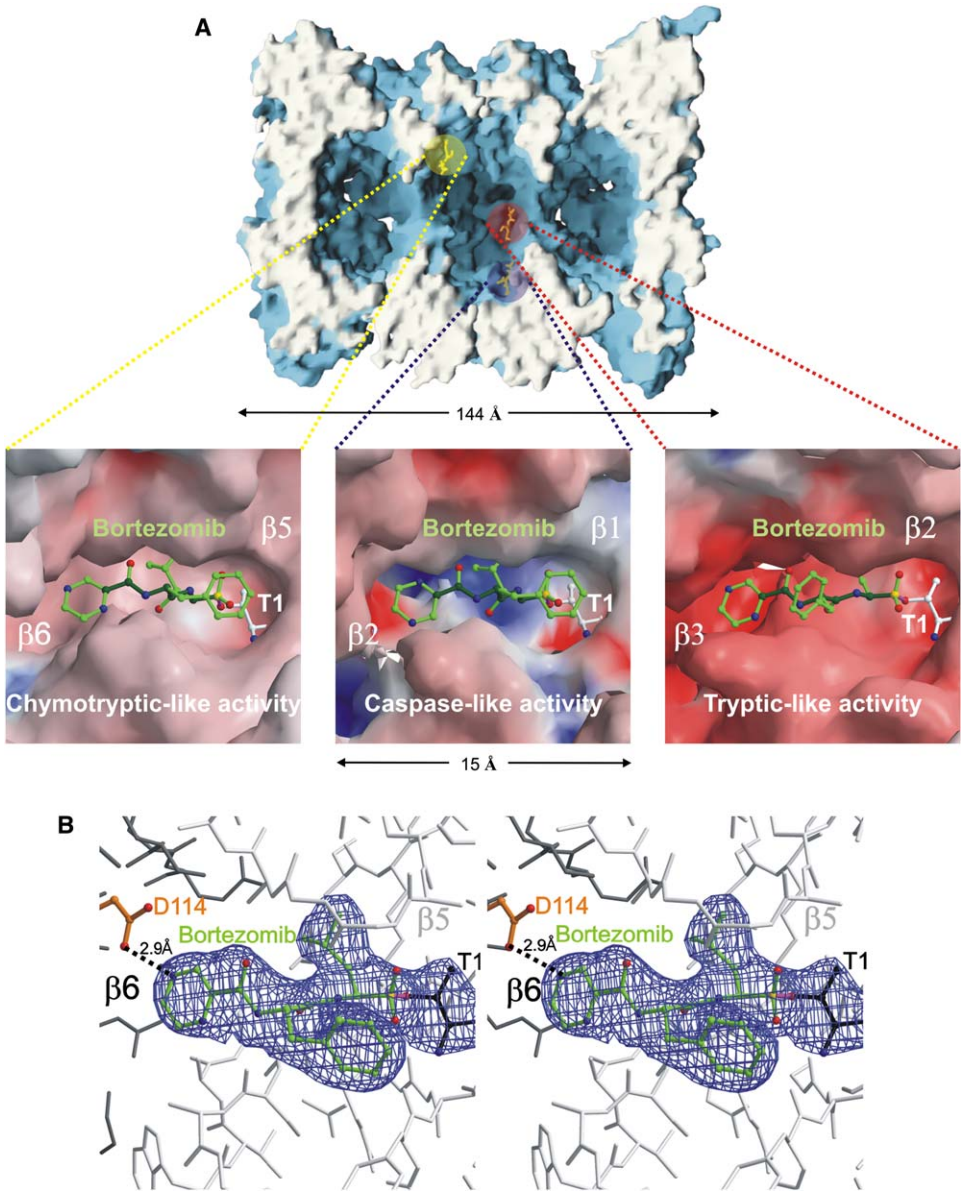

Figure 1. Structural Representation of Bortezomib Bound to Distinct Active Sites

(A) Surface representation of the yeast 20S proteasome (blue) crystallized in the presence of bortezomib, clipped along the cylindrical pseudo-7-fold symmetry axis (white). The various proteolytic surfaces are marked by a specific color coding: red = subunit β1; blue = subunit β2; and green = subunit β5. Cleavage preferences, termed chymotryptic-like, caspase-like, and tryptic-like activity, are zoomed and illustrated in surface representations; the nucleophilic threonine and bortezomib are presented as a ball-and-stick model. Basic residues are colored blue, acidic residues are red, and hydrophobic residues are white.

(B) Stereorepresentation of the chymotryptic-like active site of the yeast 20S proteasome (white and gray) and bortezomib (green). Covalent linkage of the inhibitor with the active site Thr1 of subunit β5 is drawn in pink. The electron density map (blue) is contoured from 1.2σ, with $2F_O$-F_C coefficients after 2-fold averaging. Apart from the bound inhibitor, structural changes were noted only in the specificity pockets. Temperature factor refinement indicates full occupancy of bortezomib bound to the chymotryptic-like active site. Bortezomib has been omitted for phasing.

(Figure 2). Thr21O and Ala49N, both of which are conserved in all proteolytically active centers, are essential for β sheet formation: respective carbonyl oxygen and nitrogen atoms tightly interact with bortezomib's pyrazine-2-carboxyl-phenylalanyl peptide backbone. The binding mode and conformation is uniform in all proteolytically active sites. Nonetheless, bortezomib exhibits different binding affinities to distinct active sites, due to interactions of the individual side chains of the inhibitor with protein specificity pockets.

Mechanism of Action: The Boronic Acid Moiety

The boronic acid moiety of the drug ensures increased specificity for the proteasome, as opposed to earlier generations of synthetic inhibitors, such as peptide aldehydes, which show cross-reactivity toward cysteine proteases and low metabolic stability (Vinitsky et al., 1992). The boronic acid core ensures high affinity for hard oxygen nucleophiles in contrast to soft cysteine nucleophiles, according to the Lewis hard-soft acid-base principle. As expected, the boron atom covalently interacts

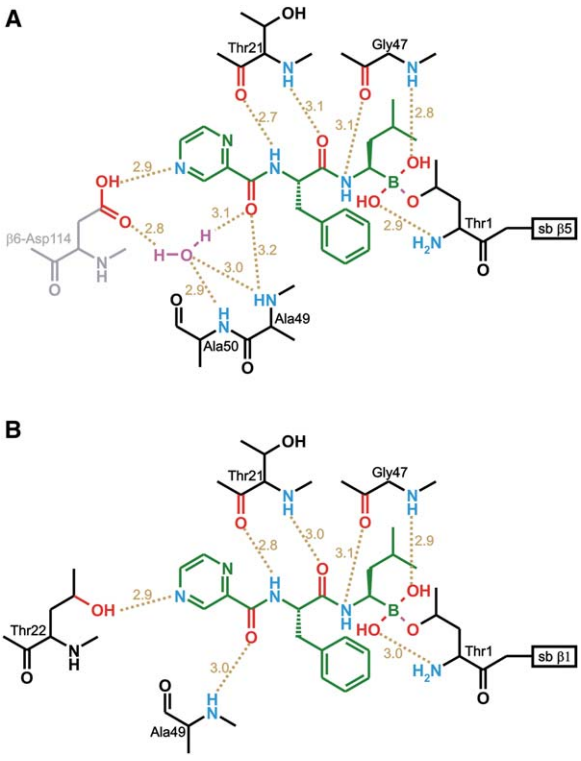

Figure 2. Critical Interactions of Bortezomib with Active Site Residues Responsible for Chymotryptic and Caspase-like Activities

Schematic overview of bortezomib bound to (A) the chymotryptic-like active site and (B) the caspase-like active site. Hydrogen bonds with correlated distances in Å are shown as brown dashed lines, whereas characteristic oxygen and nitrogen atoms are presented in red and blue capitals. The amino acid, which is responsible for the character and binding mode to the P3-pyrazine-2-carboxyl side chain of the inhibitor is located at the adjacent β-type subunit and shown in gray. The defined water molecule forming tight hydrogen bonds to the protein is depicted in magenta, and the inhibitor is shown in green.

with the nucleophilic oxygen lone pair of Thr1O$^{\gamma}$ (Figure 1B), while Gly47N, stabilizing the oxyanion hole, is hydrogen-bridged to one of the acidic boronate hydroxyl groups. The tetrahedral boronate adduct is further stabilized by a second acidic boronate hydroxyl moiety, which hydrogen-bridges the N-terminal threonine amine atom, functioning as a catalytic proton acceptor (Figure 2).

Boronic acid derivatives, and particularly peptide boronates, are well-known inhibitors of serine proteases (Walker and Lynas, 2001). Crystal structure elucidation and NMR characterization of trypsin:boronic acid complexes have revealed a covalent binding of the nucleophilic Ser195O$^{\gamma}$ to the boronic acid moiety, resulting in a serine-boronate tetrahedral transition state complex (London and Gabel, 2001; London and Gabel, 2002; Transue et al., 2004; Weber et al., 1995). Compared to serine proteases, the proteasomal active site, Thr1N, additionally forms a tight hydrogen bridge to one of the boronate hydroxyl groups, further stabilizing the protein-ligand complex, explaining the high affinity of boronic ligands to Ntn-hydrolases.

Binding to S1 Specificity Pockets: the Leucine Side Chain

Selectivity of inhibitors for proteasomal active sites can be controlled by the P1-pocket, as has been shown for lactacystin (Fenteany et al., 1995) and salinosporamides (Macherla et al., 2005), and by the P3-pocket, exemplified by vinylsulfone-inhibitors (Groll et al., 2002; Nazif and Bogyo, 2001). In vivo experiments indicated that bortezomib binds covalently with the highest affinity to the β5 subunit (Berkers et al., 2005). Our crystallographic analysis shows that bortezomib binds by inducing a fit to Met45 of subunit β5, which is involved in key enzyme-substrate interactions—in particular, those required for hydrolysis of hydrophobic peptide bonds. Compared to the crystal structure of the native unliganded proteasome, the structural data of the proteasome:bortezomib complex show that the P1-leucine side chain of the inhibitor shifts the side chain of Met45 from its original position by 2.7 Å toward Ile35. This structural rearrangement enlarges the S1-specificity pocket, engaging an induced fit, similar to what has been observed for calpain inhibitor I (Groll et al., 1997) and epoxomycin (Groll et al., 2000). Although the flexibility of side chains makes it difficult to predict optimal substitution at this site, we note that, upon ligand binding, the concerted movements allow additional hydrophobic interactions of the P1-leucine side chain of the inhibitor with residues of the S1-pocket, further stabilizing the ligand bound state.

The S1 specificity pocket of subunit β1, positively charged by Arg45, is neutralized by a counter ion, adapting to the leucyl boronic acid side chain without conformational rearrangements, as observed in the yeast proteasome:calpain inhibitor I complex (Groll et al., 1997). Subunit β1 can cleave peptide bonds after acidic and branched-chain amino acids (Groll et al., 1999; Nussbaum et al., 1998). Interactions, in particular between residues Thr20, Thr31, and Ala49 of subunit β1 and the P1 leucine side chain of bortezomib, stabilize the ligand in its bound conformation.

Bortezomib does not block the β2 active site in vivo, even in the high micromolar range. However, our structural data exhibit clear electron density of the compound covalently bound to subunit β2. The tryptic-like active site displays a large unstructured S1-specificity pocket (Groll et al., 1997), allowing for motion and flexibility of the P1-leucine side chain of the bound ligand. Although bortezomib adopts a β-conformation in the tryptic-like active site, similar to that observed for subunits β1 and β5 (Figure 1A), its P1-leucine side chain does not form hydrophobic interactions with residues of the S1 specificity pocket. The probability of covalent binding of bortezomib to the various active site threonine residues correlates well with the affinities of the ligand for the individual binding clefts. Low binding affinity of the boronic P1-leucine side chain to the S1 pocket may lead to a reduced occupancy of bortezomib in the tryptic-like active site, thus increasing its IC_{50} value.

Binding to S2 Pockets by the Phenylalanine Residue

The phenylalanine moiety of bortezomib is not in contact with the protein, and points into empty space. Thus, the S2 pockets of all active sites are able to accept space-demanding side chain residues because of their unique topology. However, our structural data show that the conformation of the P2-phenylalanine side chain of bortezomib is flipped in the tryptic-like active site relative to its conformation in the chymotryptic and caspase-like active sites (Figure 1A). This result is surprising, since

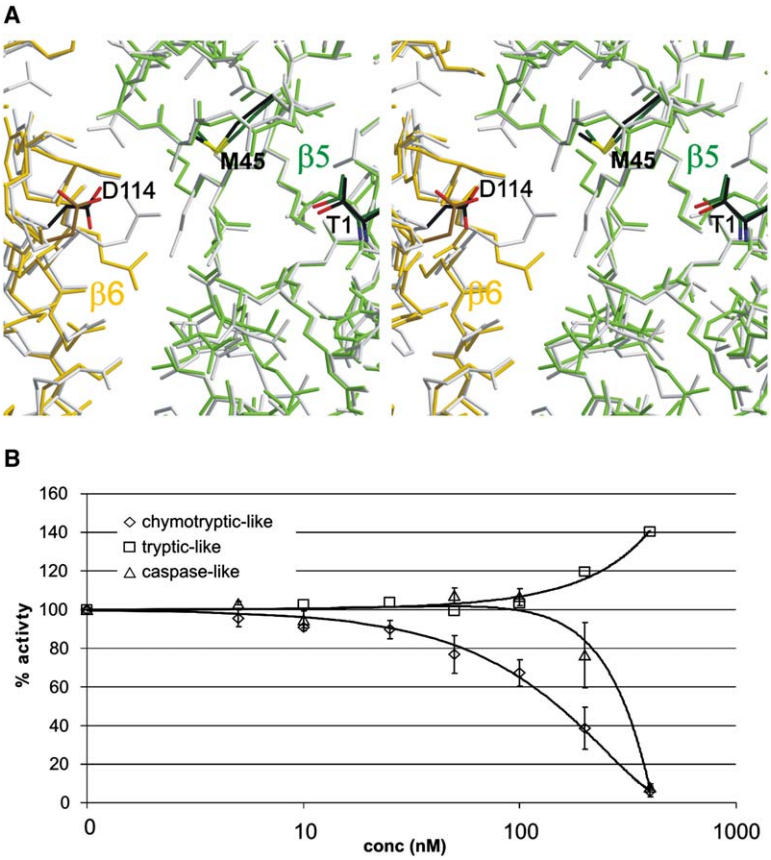

Figure 3. Comparison of Yeast and Mammalian Proteasomes

(A) Stereoview of the superposition of the β5 and β6 subunits of native bovine and yeast proteasome. The yeast β5 and β6 subunits are colored green and yellow, respectively, whereas subunits of the bovine liver proteasome are colored gray. Residues, which in particular regulate the character of the S1 and S3 pocket (Met45 and Asp114) are colored black, as well as the active site threonine residues.

(B) Individual catalytic activities of the yeast 20S proteasome against small fluorogenic peptide substrates upon treatment with bortezomib. The tryptic-like activity shows increased activity at high concentrations of bortezomib, an unexplained phenomenon observed previously. Error bars represent ± 1 SEM.

both conformations of the P2-phenylalanine side chain of bortezomib would fit in the three distinct specificity pockets of the various proteolytically active sites without making contact with protein residues. Thus, the P2 site of bortezomib possibly contributes to overall pharmacodynamic properties, but surely not to kinetics of inhibition. Presumably, specific gain may be obtained by the introduction of large hydrophobic moieties at the P2-site (Braun et al., 2005; Elofsson et al., 1999, Harris et al., 2001; Kisselev et al., 2003; Nazif and Bogyo, 2001).

Binding Probabilities of Bortezomib by the Pyrazine-2-carboxyl Group

Specific interactions are formed between the pyrazine-2-carboxyl side chain of bortezomib and residues of the subunit-specific S3 pockets. In the case of the chymotryptic-like active site, the P3 pyrazine ring is hydrogen-bridged to the hydroxyl group of Asp114 of the adjacent β6 subunit. Only one of the nitrogen atoms of the pyrazine residue is stabilized, but the observed interaction is strong, as evidenced by the short bond length of 2.9 Å. The experimental electron density reveals a well-defined water molecule in proximity to Asp114O$^{\gamma}$, which coordinates a tight hydrogen bonding network, interacting with β6Asp114O$^{\gamma}$, β5Ala49N, and β5Ala50N of the protein and with the carbonyl oxygen of bortezomib (Figure 2A). In the case of caspase-like activity, the pyrazine-2-carboxyl side chain is only hydrogen bridged to Thr22O$^{\gamma}$ of subunit β1 (2.9 Å). Position 114 of the neighboring subunit β2 displays a histidine residue that does not interact with the pyrazine ring. Therefore, only the carbonyl oxygen of β1Ala40 stabilizes the peptide backbone of bortezomib by formation of the β conformation, whereas a defined water molecule, present in the chymotryptic-like active site, is absent in the caspase-like active site (Figure 2B). Important interactions of the pyrazine ring of β2 bound bortezomib are lacking in the tryptic-like active site. Although an aspartic residue is present at position 114 of the adjacent subunit β3, with similar orientations as described for the chymotryptic-like active site, the S3 binding pockets of these two proteolytically active sites differ significantly, thus providing further explanation for the subunit selectivity of bortezomib. Upon closer inspection of the pyrazine moiety, it becomes evident that the P3 site is also critical for the high affinity of bortezomib to the chymotryptic-like active site. Thus, alterations to the P1 and/or P3 sites may significantly improve binding properties of the drug to the respective proteolytically active sites (Elofsson et al., 1999; Harris et al., 2001; Kisselev et al., 2003; Nazif and Bogyo, 2001).

Discussion

Here we report the crystal structure of the yeast 20S proteasome in complex with bortezomib. The clinical use of this agent makes it imperative that its binding mode to mammalian proteasomes be established, not only to fully understand its mechanism of inhibition, but also to provide a platform for rational improvements in specificity and strength of inhibition. The structural superposition of bovine liver (Unno et al., 2002) and yeast (Groll et al., 1997) proteasomes shows the expected high degree of structural similarity, despite crystallization in

different space groups, as illustrated in Figure 3, by subunits β5 and β6 of the bovine and yeast CP. The ability of bortezomib to inhibit individual subunits of the yeast 20S proteasome is consistent with kinetic data obtained for mammalian proteasomes (Berkers et al., 2005; Lightcap et al., 2000). This is shown by independent measurements of catalytic activities of the yeast 20S proteasome upon treatment with bortezomib as observed using fluorogenic substrates in the absence of sodium dodecylsulfate or activators (Figure 3B). So far, biochemical and crystallographic characterization of active site mutants has been performed only in yeast (Chen and Hochstrasser, 1996; Heinemeyer et al., 1997; Jager et al., 1999). Mutagenic inactivation of proteasomal active site residues has revealed some striking phenotypes. In particular, the Thr1:Ala mutation of the active site subunit β5 is lethal, and the Lys33:Ala mutation causes severe growth defects, whereas the β1Thr1:Ala and β2Thr1:Ala active site mutations are less toxic. It is therefore important to understand the physiological contributions of single proteasomal subunits in the mammalian system, which can be addressed by specific, subunit-selective and cell-permeable proteasome inhibitors. The crystal structure of bortezomib bound to the yeast 20S proteasome illustrates concerted movements that affect binding affinities of the inhibitor to the proteolytic active sites.

Since bortezomib is now used for the treatment of the universally fatal hematologic malignancy multiple myeloma (Richardson et al., 2005), with clinical trials for other malignancies ongoing, it is imperative to establish its mode of action at the molecular level. The structural data for the bortezomib-proteasome complex presented here explain the different in vivo binding affinities of bortezomib for the individual subunits at atomic resolution. Our data immediately suggest possibilities for the design of bortezomib derivatives with superior inhibition characteristics, and for the design of inhibitors that will specifically bind to single proteolytically active sites. Thus, the crystal structure of this 20S-bortezomib complex may serve as a new lead for rational design of selective boronic acid-based proteasome inhibitors.

Experimental Procedures

Cocrystallization

Crystals of 20S proteasome from *Saccharomyces cerevisiae* were grown in hanging drops at 24ºC, as described previously (Groll and Huber, 2005), and incubated for 60 min with bortezomib (10 mM in DMSO), which was synthesized essentially as described previously (Adams et al., 1998). The protein concentration used for crystallization was 40 mg/ml in Tris-HCl (10 mM, pH 7.5) and EDTA (1 mM). Drops contained 3 μl of protein and 2 μl of reservoir solution (30 mM MgOAc, 100 mM morpholino-ethane-sulphonic acid [MES, pH 7.2], and 10% 2-methyl-2,4-pentanediol [MPD]).

The space group of proteasomal complex crystals belongs to $P2_1$, with cell dimensions of a = 136.2 Å, b = 300.7 Å, c = 144.7 Å, and β = 113.3º. Data to 2.8 Å were collected using synchrotron radiation with λ = 1.05 Å at the BW6-beamline at DESY, Hamburg, Germany. Crystals were soaked in a cryoprotecting buffer (30% MPD, 20 mM MgOAc, 100 mM MES, pH 6.9) and frozen in a stream of liquid nitrogen gas at 90K (Oxford Cryo Systems). X-ray intensities were evaluated using the DENZO program and data reduction was performed with SCALEPACK (Otwinowski et al., 2003; Otwinowski and Minor, 1997). Anisotropy of diffraction was corrected by an overall anisotropic temperature factor, comparing observed and calculated structure amplitudes using the program CNS (Brünger et al., 1998). A total of 4,253,531 reflections yielded 249,075 unique reflections (96.5% completeness). The corresponding R_{merge} was 9.1% at 2.8 Å resolution (44.2% for the last resolution shell). Electron density was improved by averaging and back-transforming reflections 10 times over the 2-fold noncrystallographic symmetry axis using the program MAIN (Turk, 1992). Conventional crystallographic rigid body, positional, and temperature factor refinements were carried out with CNS using the yeast 20S proteasome structure as starting model (Groll et al., 1997). For model building, the program MAIN was used. The structure was refined to a crystallographic R-factor of 23.1% (free R factor, 26.4%; Brünger, 1993), with rmsds from target values of 0.007 Å for bonds and 1.33º for angles (Engh and Huber, 1991). Modeling experiments were performed using the coordinates of yeast 20S proteasome (Groll et al., 1997) with the program MAIN.

Proteasome Activity Assay with Fluorogenic Substrates

Assays were performed as previously described (Elliott et al., 2003) with minor changes. Proteasome (100 μg/ml) was incubated with various concentrations of bortezomib for 1 hr at 37ºC. An aliquot of 1 μg was added to 100 μl of substrate buffer, containing 20 mM HEPES (pH 8.2), 0.5 mM EDTA, 1% DMSO, and 180 μM BzValGlyArgAMC (tryptic-like activity, β2), 100 μM SucLeuLeuValTyrAMC (chymotryptic-like activity β5), or 180 μM ZLeuLeuGlu-βNA (caspase-like activity β1). SDS was omitted from the substrate buffer. Fluorescence was measured every minute for 35 min at 37ºC using a Fluostar Optima 96-well plate reader (BMG Labtechnologies) ($\lambda_{ex}/\lambda_{em}$ = 355/450 nm for AMC and 320/405 nm for βNA), and the increase in fluorescence per minute was used to calculate specific activities of each sample.

Acknowledgments

We are grateful to Gleb Bourenkov for his valuable help during crystal measurements at the Deutsche Electronen Synchrotron facilities in Hamburg. This work was supported by grants from The Netherlands Organization for Scientific Research (NWO) and the Dutch Cancer Society (KWF) to H.O., and by support from the NIH to H.P.

Received: October 7, 2005
Revised: November 16, 2005
Accepted: November 17, 2005
Published online: March 14, 2006

References

Adams, J., Behnke, M., Chen, S., Cruickshank, A.A., Dick, L.R., Grenier, L., Klunder, J.M., Ma, Y.T., Plamondon, L., and Stein, R.L. (1998). Potent and selective inhibitors of the proteasome: dipeptidyl boronic acids. Bioorg. Med. Chem. Lett. *8*, 333–338.

Berkers, C.R., Verdoes, M., Lichtman, E., Fiebiger, E., Kessler, B.M., Anderson, K.C., Ploegh, H.L., Ovaa, H., and Galardy, P.J. (2005). Activity probe for in vivo profiling of the specificity of proteasome inhibitor bortezomib. Nat. Methods *2*, 357–362.

Brannigan, J.A., Dodson, G., Duggleby, H.J., Moody, P.C., Smith, J.L., Tomchick, D.R., and Murzin, A.G. (1995). A protein catalytic framework with an N-terminal nucleophile is capable of self-activation. Nature *378*, 416–419.

Braun, H.A., Umbreen, S., Groll, M., Kuckelkorn, U., Mlynarczuk, I., Wigand, M.E., Drung, I., Kloetzel, P.M., and Schmidt, B. (2005). Tripeptide mimetics inhibit the 20 S proteasome by covalent bonding to the active threonines. J. Biol. Chem. *280*, 28394–28401.

Brünger, A.T. (1993). Assessment of phase accuracy by cross validation: the free R value. Methods and applications. Acta Crystallogr. D Biol. Crystallogr. *49*, 24–36.

Brünger, A., Adams, P., Clore, G., DeLano, W., Gros, P., Grosse-Kunstleve, R., Jiang, J., Kuszewski, J., Nilges, M., Pannu, N., et al. (1998). Crystallography & NMR system: a new software suite for macromolecular structure determination. Acta Crystallogr. D Biol. Crystallogr. *1*, 905–921.

Chen, P., and Hochstrasser, M. (1996). Autocatalytic subunit processing couples active site formation in the 20S proteasome to completion of assembly. Cell *86*, 961–972.

Elliott, P.J., Soucy, T.A., Pien, C.S., Adams, J., and Lightcap, E.S. (2003). Assays for proteasome inhibition. Methods Mol. Med. *85*, 163–172.

Elofsson, M., Splittgerber, U., Myung, J., Mohan, R., and Crews, C.M. (1999). Towards subunit-specific proteasome inhibitors: synthesis and evaluation of peptide alpha′,beta′-epoxyketones. Chem. Biol. *6*, 811–822.

Engh, R., and Huber, R. (1991). Accurate bond and angles parameters for X-ray protein structure refinement. Acta Crystallogr. A *47*, 392–400.

Fenteany, G., Standaert, R.F., Lane, W.S., Choi, S., Corey, E.J., and Schreiber, S.L. (1995). Inhibition of proteasome activities and subunit-specific amino-terminal threonine modification by lactacystin. Science *268*, 726–731.

Groll, M., and Huber, R. (2004). Inhibitors of the eukaryotic 20S proteasome core particle: a structural approach. Biochim. Biophys. Acta *1695*, 33–44.

Groll, M., and Huber, R. (2005). Purification, crystallization and X-ray analysis of the yeast 20S proteasomes. Methods Enzymol. *398*, 329–336.

Groll, M., Ditzel, L., Lowe, J., Stock, D., Bochtler, M., Bartunik, H.D., and Huber, R. (1997). Structure of 20S proteasome from yeast at 2.4 Å resolution. Nature *386*, 463–471.

Groll, M., Heinemeyer, W., Jager, S., Ullrich, T., Bochtler, M., Wolf, D.H., and Huber, R. (1999). The catalytic sites of 20S proteasomes and their role in subunit maturation: a mutational and crystallographic study. Proc. Natl. Acad. Sci. USA *96*, 10976–10983.

Groll, M., Kim, K.B., Kairies, N., Huber, R., and Crews, C.M. (2000). Crystal structure of epoxomicin: 20S proteasome reveals a molecular basis for selectivity of alpha′,beta′-epoxyketone proteasome inhibitors. J. Am. Chem. Soc. *122*, 1237–1238.

Groll, M., Nazif, T., Huber, R., and Bogyo, M. (2002). Probing structural determinants distal to the site of hydrolysis that control substrate specificity of the 20S proteasome. Chem. Biol. *9*, 655–662.

Groll, M., Bochtler, M., Brandstetter, H., Clausen, T., and Huber, R. (2005). Molecular machines for protein degradation. ChemBioChem *6*, 222–256.

Harris, J.L., Alper, P.B., Li, J., Rechsteiner, M., and Backes, B.J. (2001). Substrate specificity of the human proteasome. Chem. Biol. *8*, 1131–1141.

Heinemeyer, W., Fischer, M., Krimmer, T., Stachon, U., and Wolf, D.H. (1997). The active sites of the eukaryotic 20 S proteasome and their involvement in subunit precursor processing. J. Biol. Chem. *272*, 25200–25209.

Hershko, A., and Ciechanover, A. (1998). The ubiquitin system. Annu. Rev. Biochem. *67*, 425–479.

Jager, S., Groll, M., Huber, R., Wolf, D.H., and Heinemeyer, W. (1999). Proteasome beta-type subunits: unequal roles of propeptides in core particle maturation and a hierarchy of active site function. J. Mol. Biol. *291*, 997–1013.

Kisselev, A.F., and Goldberg, A.L. (2001). Proteasome inhibitors: from research tools to drug candidates. Chem. Biol. *8*, 739–758.

Kisselev, A.F., Garcia-Calvo, M., Overkleeft, H.S., Peterson, E., Pennington, M.W., Ploegh, H.L., Thornberry, N.A., and Goldberg, A.L. (2003). The caspase-like sites of proteasomes, their substrate specificity, new inhibitors and substrates, and allosteric interactions with the trypsin-like sites. J. Biol. Chem. *278*, 35869–35877.

Lightcap, E.S., McCormack, T.A., Pien, C.S., Chau, V., Adams, J., and Elliott, P.J. (2000). Proteasome inhibition measurements: clinical application. Clin. Chem. *46*, 673–683.

London, R.E., and Gabel, S.A. (2001). Development and evaluation of a boronate inhibitor of gamma-glutamyl transpeptidase. Arch. Biochem. Biophys. *385*, 250–258.

London, R.E., and Gabel, S.A. (2002). Formation of a trypsin-borate-4-aminobutanol ternary complex. Biochemistry *41*, 5963–5967.

Löwe, J., Stock, D., Jap, B., Zwickl, P., Baumeister, W., and Huber, R. (1995). Crystal structure of the 20S proteasome from the archaeon *T. acidophilum* at 3.4 Å resolution. Science *268*, 533–539.

Ludwig, H., Khayat, D., Giaccone, G., and Facon, T. (2005). Proteasome inhibition and its clinical prospects in the treatment of hematologic and solid malignancies. Cancer. *104*, 1794–1807.

Macherla, V.R., Mitchell, S.S., Manam, R.R., Reed, K.A., Chao, T.H., Nicholson, B., Deyanat-Yazdi, G., Mai, B., Jensen, P.R., Fenical, W.F., et al. (2005). Structure-activity relationship studies of salinosporamide A (NPI-0052), a novel marine derived proteasome inhibitor. J. Med. Chem. *48*, 3684–3687.

Nazif, T., and Bogyo, M. (2001). Global analysis of proteasomal substrate specificity using positional-scanning libraries of covalent inhibitors. Proc. Natl. Acad. Sci. USA *98*, 2967–2972.

Nussbaum, A.K., Dick, T.P., Keilholz, W., Schirle, M., Stevanovic, S., Dietz, K., Heinemeyer, W., Groll, M., Wolf, D.H., Huber, R., et al. (1998). Cleavage motifs of the yeast 20S proteasome beta subunits deduced from digests of enolase 1. Proc. Natl. Acad. Sci. USA *95*, 12504–12509.

Orlowski, M., Cardozo, C., and Michaud, C. (1993). Evidence for the presence of five distinct proteolytic components in the pituitary multicatalytic proteinase complex: properties of two components cleaving bonds on the carboxyl side of branched chain and small neutral amino acids. Biochemistry *32*, 1563–1572.

Otwinowski, Z., and Minor, W. (1997). Processing of X-ray diffraction data collected in oscillation mode. Methods Enzymol. *276*, 307–326.

Otwinowski, Z., Borek, D., Majewski, W., and Minor, W. (2003). Multiparametric scaling of diffraction intensities. Acta Crystallogr. A *59*, 228–234.

Richardson, P.G., Sonneveld, P., Schuster, M.W., Irwin, D., Stadtmauer, E.A., Facon, T., Harousseau, J.L., Ben-Yehuda, D., Lonial, S., Goldschmidt, H., et al. (2005). Bortezomib or high-dose dexamethasone for relapsed multiple myeloma. N. Engl. J. Med. *352*, 2487–2498.

Teicher, B.A., Ara, G., Herbst, R., Palombella, V.J., and Adams, J. (1999). The proteasome inhibitor PS-341 in cancer therapy. Clin. Cancer Res. *5*, 2638–2645.

Transue, T.R., Krahn, J.M., Gabel, S.A., DeRose, E.F., and London, R.E. (2004). X-ray and NMR characterization of covalent complexes of trypsin, borate, and alcohols. Biochemistry *43*, 2829–2839.

Turk, D. (1992). Improvement of a programm for molecular graphics and manipulation of electron densities and its application for protein structure determination. Thesis, Technische Universitaet Muenchen, Germany.

Unno, M., Mizushima, T., Morimoto, Y., Tomisugi, Y., Tanaka, K., Yasuoka, N., and Tsukihara, T. (2002). The structure of the mammalian 20s proteasome at 2.75 Å resolution. Structure *10*, 609–618.

Vinitsky, A., Michaud, C., Powers, J.C., and Orlowski, M. (1992). Inhibition of the chymotrypsin-like activity of the pituitary multicatalytic proteinase complex. Biochemistry *31*, 9421–9428.

Walker, B., and Lynas, J.F. (2001). Strategies for the inhibition of serine proteases. Cell. Mol. Life Sci. *58*, 596–624.

Weber, P.C., Lee, S.L., Lewandowski, F.A., Schadt, M.C., Chang, C.W., and Kettner, C.A. (1995). Kinetic and crystallographic studies of thrombin with Ac-(D)Phe-Pro-boroArg-OH and its lysine, amidine, homolysine, and ornithine analogs. Biochemistry *34*, 3750–3757.

Accession Numbers

Coordinates have been deposited in the RCSB Protein Data Bank under the accession code 2F16.